Astronomy & Astrophysics

H₂O maser emission from bright rimmed clouds in the southern hemisphere⋆

R. Valdettaro[1], J. M. Chapman[2], J. E. J. Lovell[2,3], and F. Palla[1]

[1] INAF – Osservatorio Astrofisico di Arcetri, Largo E. Fermi 5, 50125 Firenze, Italy
  e-mail: rv@arcetri.astro.it
[2] CSIRO Australia Telescope National Facility, PO Box 76, Epping, NSW 1710, Australia
[3] CSIRO Industrial Physics, PO Box 218, Lindfield NSW 2070

ABSTRACT

Context. Water maser emission is a powerful tracer of the presence of embedded sources in dense clouds since it requires elevated temperatures (>100 K) and densities ($>10^7$ cm^{-3}) that can be found in circumstellar disks and/or jets/outflows associated with Young Stellar Objects. Bright rimmed clouds compressed by ionization fronts from nearby massive stars are considered good examples of externally triggered star formation, possibly resulting in the formation of massive stars.
Aims. We aim to determine the water maser emission frequency and characteristics of 45 bright rimmed clouds in the southern hemisphere identified by Sugitani & Ogura (1994, ApJS, 92, 163).
Methods. We have used the Tidbinbilla 70-m radiotelescope to perform a high sensitivity survey at 22.2 GHz of the maser emission from the $6_{16}-5_{23}$ rotational transition of H₂O molecules.
Results. We found 7 water maser sources out of 44 (16% detection rate), 5 being new detections. With the exception of the maser associated with BRC 68, all the other maser are characterized by low integrated fluxes and luminosities.
Conclusions. Most maser sources fall below the correlation between the H₂O and far-infrared luminosity found in other studies towards a variety of star forming regions. These results are similar to those found in the companion survey of BRCs in the northern hemisphere by Valdettaro et al. (2005, A&A, 443, 535). The low detection frequency and the properties of water maser emission from BRCs indicate that low-mass star formation is the most natural outcome of the external compression induced by the ionization front from nearby massive stars.

Key words. ISM: clouds – masers – stars: formation – radio lines: ISM

1. Introduction

Clouds in the interstellar medium can be compressed by an external ionization-shock front which can concentrate the neutral gas into compact globules (Bertoldi 1989). The boundary layer between the neutral gas and the denser gas ionized by the incident photons is often called a "bright rim" (Tauber et al. 1993), but the clumps are sometimes classified also as "speck" or "cometary" globules depending on their appearance (e.g. Leung 1985). After Reipurth (1983) reported some evidence for the presence of young stars embedded in the bright-rimmed source CG 1, small globules with bright rims have been considered potential sites of star formation, possibly triggered by the external compression.

Catalogs of optically selected bright-rimmed clouds (BRCs) associated with IRAS point sources have been presented by Sugitani et al. (1991) for the northern hemisphere and by Sugitani & Ogura (1994) for the southern hemisphere. Searches for these BRCs were made using the Palomar Observatory Sky Survey (POSS) prints for the northern sky and the ESO (R)/SERC (J) atlases for the southern sky. A total of 89 BRCs, 44 in the northern hemisphere and 45 in the southern hemisphere, were identified and catalogued by Sugitani and collaborators. These authors noted that the ratio of the

luminosity of the IRAS source to the globule mass (as measured from molecular line emission) appeared to be much higher in BRCs than in isolated dark clouds/globules. This result prompted the suggestion that star formation may proceed in a different mode in globules associated with bright rims than in more quiescent and isolated ones, resulting in the production of more luminous, hence massive stars. Later studies have confirmed the presence in some BRCs of small clusters of embedded sources of intermediate and high far infrared luminosity ($L_{FIR} > 10^2$ $L_\odot$, Sugitani et al. 1995). However, a complete census of the properties of the embedded stellar population is still lacking and the question of whether induced star formation actually takes place in most/all of the BRCs has only been partially answered.

A reliable diagnostic of the presence of newly formed young stellar objects (YSOs) in dense cores is the detection of 22.2 GHz H₂O maser emission. The physical conditions near YSOs, characterized by high temperatures (>100 K) and densities ($>10^7$ cm^{-3}) are suitable for maser excitation and indeed maser emission has been detected in association with both low- and high-mass YSOs (e.g., Furuya et al. 2003; Trinidad et al. 2003; Healy et al. 2004; Goddi et al. 2005). Also, since maser spots are distributed close to the exciting source (spatial scales of 1–100 AU) either along the jet/outflow or in a circumstellar disk, they provide a unique opportunity to investigate the physics of these regions, (e.g., Cesaroni 2005; Moscadelli et al. 2005;

⋆ Based on observations obtained with the 70-m Tidbinbilla radiotelescope.

Goddi & Moscadelli 2006). Taking advantage of this basic property of water masers, we have performed multi-epoch observations of the 44 northern BRCs listed by Sugitani et al. (1991) using the Medicina radio-telescope at 22.2 GHz. The survey had a rather limited sensitivity with a typical rms of 1 Jy and resulted in the detection of only three water masers, two being first detections (Valdettaro et al. 2005). Since the frequency of occurrence of water masers is higher towards bright IRAS sources and decreases substantially at lower luminosity (Palla et al. 1991, 1993), the negative result of the Medicina survey was somewhat surprising, if the suggestion of induced intermediate/high-mass star formation is indeed correct. As a possible explanation, we argued that either the external compression does not favor gravitational collapse and star formation or that BRCs mostly produce low-luminosity objects in which the frequency of occurrence of water maser is low and highly episodic (e.g., Claussen et al. 1996; Valdettaro et al. 2003; Brand et al. 2005). This conclusion was also reached by Healy et al. (2004) in their high spatial resolution VLA study of the water maser distribution in several HII regions. Finally, the possibility exists that the YSOs embedded in BRCs are in a more advanced evolutionary phase than protostars (Class 0 sources; André et al. 1993), since it is also well known that the maser activity decreases systematically with time/evolutionary stage (e.g. Furuya et al. 2001, 2003).

In order to test the initial results obtained in the northern hemisphere, we have carried out a survey of the 45 southern BRCs of Sugitani & Ogura (1994) using the Tidbinbilla 70-m antenna. The rms detection levels were typically 110 mJy, a factor of ~10 more sensitive than the Medicina survey.

2. Observations

Observations of the maser emission from the $6_{16} - 5_{23}$ rotational transition of water at 22.235080 GHz were taken as service observations with the Tidbinbilla DSS43 70-m antenna in several sessions between April 2003 and February 2005. At the frequency of the H_2O transition, the Tidbinbilla antenna has a HPBW of ~39 arcsec and the average pointing error was typically ~4 arcsec. A total bandwidth of 32 MHz was chosen with 2049 spectral channels across the bandpass, giving a total velocity coverage of 430 km s^{-1} and a spectral resolution of 0.25 km s^{-1}. The peak sensitivity of the Tidbinbilla antenna, at 22 GHz, is ~1.5 Jy/K. Spectra were taken in position-switching mode with integration times of 5 min both on- and off-source. Flux calibration was derived from antenna temperature measurements at different elevations of PKS 1830−211 (6.3 ± 0.3 Jy) and PKS 1921−293 (10.9 ± 0.4 Jy). These flux densities were calibrated against observations of 3C286, with an absolute flux density for 3C286 of 2.6 Jy at a frequency of 21.8 GHz. The calibration uncertainty is estimated to be ~10%.

Fourty four of the 45 sources have been observed at least once and some two or three times. The typical rms noise level for all spectra is ~65 mK, or ~110 mJy. For sources with no detections, the 5σ upper limits are about 0.55 Jy. The list of the southern BRCs with the corresponding IRAS source, observing date, and individual rms is given in Table 1. For one source, BRC 75 (IRAS 15519−5430), the observations taken cannot be used as the antenna elevation was too low. We therefore exclude this source from further discussion.

Initial data reduction to calculate quotient spectra and determine the velocity scale was done using SPC, a single-dish spectral line data reduction package supported by the Australia National Telescope Facility. Further reduction to fit baselines,

Table 1. H_2O maser observations of Bright Rimmed Clouds. BRCs with water maser emission are in boldface.

BRC #	IRAS source	Observation date (dd/mm/yy)	rms (mJy)
45	07162−2200	07/04/03	85
46	07178−4429	07/04/03, 10/04/03	85, 85
47	07296−1921	07/04/03	85
48	07329−4647	07/04/03, 08/04/03	85, 90
49	07334−1842	10/04/03	85
50	07388−4259	07/04/03	85
51	08076−3556	10/04/03	85
52	08242−5050	07/04/03	85
53	08250−5030	07/04/03	85
54	08337−4028	07/04/03, 08/04/03, 12/05/03	85, 90, 170
55	08393−4041	13/06/03, 27/08/03	60, 60
56	08411−3949	07/04/03	90
57	08423−4105	07/04/03	85
58	08435−4105	07/04/03, 10/04/03	85, 85
59	08563−4711	07/04/03	85
60	08583−4719	07/04/03, 10/04/03	85, 85
61	10581−5920	10/04/03	85
62	10591−5934	10/04/03	85
63	11012−5931	10/04/03, 30/04/03	85, 105
64	11101−5829	10/04/03, 30/04/03	85, 105
65	11306−6311	10/04/03, 30/04/03	85, 105
66	11315−6259	10/04/03, 30/04/03	85, 105
67	11317−6254	10/04/03, 30/04/03	85, 105
68	11332−6258	30/04/03	105
69	11388−6306	30/04/03	105
70	11398−6251	30/04/03, 27/08/03	105, 60
71	13050−6154	30/04/03	105
72	13158−6217	30/04/03	105
73	13168−6208	30/04/03	105
74	14159−6111	12/05/03, 14/02/05	170, 130
75	15519−5430	12/05/03	poor data
76	16069−4858	14/02/05	130
77	16168−2526	14/02/05	130
78	16178−2501	14/02/05	130
79	16362−4845	14/02/05	130
80	16365−4836	14/02/05	130
81	16373−4911	14/02/05	130
82	16438−4110	14/02/05	130
83	16487−4043	14/02/05	130
84	16502−4002	14/02/05	130
85	16555−4237	14/02/05	130
86	17463−3128	20/05/04, 14/02/05	130, 130
87	17597−2422	20/05/04, 14/02/05	130, 130
88	18012−2407	20/05/04, 14/02/05	130, 130
89	18068−2405	20/05/04, 14/02/05	130, 130

apply flux calibration and measure spectra, was done using the Spectral Line Analysis Package (SLAP, Staveley-Smith 1985).

3. Results

Water maser emission has been detected in 7 southern BRCs, five of which represent first time detection. The main parameters of the detected sources are listed in Table 2 that gives the BRC number following Sugitani & Ogura (1994) (Col. 1), the IRAS source (Col. 2), the observing date (Col. 3), the spectral resolution (Col. 4), the 1σ rms (Col. 5), the minimum and maximum of the velocity interval where emission is observed (Cols. 6–7), the velocity of the peak flux component (Col. 8), the total integrated H_2O flux density (Col. 9). Below, we give a brief description of the maser environment and of the main features of the maser emission for each detected BRC.

Table 2. Main parameters of the H$_2$O maser emission.

#	IRAS	Date	ΔV (km s^{-1})	rms (mJy)	V_{min} (km s^{-1})	V_{max} (km s^{-1})	V_{peak} (km s^{-1})	$\int F_\nu dV$ (Jy km s^{-1})
55	08393−4041	13/06/03	20	52	−8.0	+10	+2.48	58.0
		27/08/03	20	56	−8.4	+9.6	+1.30	51.9
64	11101−5829	10/04/03	99	82	−51	+42	−17.4	21.9
		30/04/03	69	96	−42	+28	−15.2	17.7
66	11315−6259	10/04/03	20	87	−18.9	+2.6	+0.49	1.0
		30/04/03	<2	110	−1.0	+0.8	+0.54	1.4
68	11332−6258	30/04/03	13	102	−21.5	−8.7	−12.6	480.2
71	13050−6154	30/04/03	<2	106	−43.2	−40.7	−41.8	6.5
76	16069−4858	14/02/05	3	126	−26	−23	−25.0	2.2
79	16362−4845	14/02/05	<2	130	+7.7	+12.1	+10.9	4.5

3.1. BRC 55, SFO 55, IRAS 08393–4041, G260.8+00.7

This is part of the Vela Molecular Ridge at a distance of 700 ± 200 pc (Massi et al. 1999). The relatively bright IRAS source, L_{FIR} = 510 $L_\odot$, belongs to the VMR-D cloud, according to the designation of Murphy & May (1991), which is part of an extensive network of CO clouds, corresponding to region 8 in Yamaguchi et al. (1999). The BRC is illuminated by the O7 star vBH 17a that is the source exciting the H II region NGC 2626. In a detailed NIR study of the embedded population, Massi et al. (1999) conclude that the IRAS ellipse does not contain point sources and that only one NIR source (n.21) is tentatively identified as a possible counterpart to the IRAS source. Unlike other IRAS sources in the region, this one shows only a moderate clustering of NIR sources. No radio emission at 20 cm down to an rms of 0.5 mJy/beam has been detected by Thompson et al. (2004).

The source was observed on two occasions and maser emission was detected in both cases. Spectra of the water maser emission for BRC 55 are shown in Fig. 1. The emission shows multiple components, extending over a velocity interval of about 20 km s^{-1} and centered at $V_{H_2O} \sim 2$ km s^{-1}, slightly offset from the cloud velocity of V_{cl} = +7.6 km s^{-1} (see Table 3). The individual spectral features varied strongly between June and August 2003, although the overall velocity range was essentially the same. Both spectra have the best rms (60 mJy) of our observations and do not show weak features away from the bright lines. The integrated flux is about the same in two observations, yielding a total luminosity of $L_{H_2O} = 6.6 \times 10^{-7}$ $L_\odot$.

3.2. BRC 64, SFO 64, IRAS 11101–5829, G.290.4+01.7

Yamaguchi et al. (1999, Region 12) find 2 molecular clouds associated with BBW 347. There is a strong IRAS source located close to the bright rim with $L_{FIR} = 1.4 \times 10^4$ $L_\odot$, assuming a distance of 2.7 kpc (Ogura & Walsh 1991). The IRAS source is associated with the Herbig-Haro objects 135 and 136, and presumably is the exciting source of the flow (Tamura et al. 1997). OH and H$_2$O maser emission was reported by Braz et al. (1989), while Walsh et al. (1997) have detected a methanol maser at the same location. Radio emission at 13 and 20 cm with flux density of 117 and 236 mJy, respectively, has been detected by Thompson et al. (2004), coincident with the position of the optical rim.

The source was observed in two observations in April 2003, separated by 20 days, and maser emission was detected on both occasions. As shown in Fig. 2, there are several components that cover a large velocity interval of about 90 km s^{-1}. The main component has a peak value varying between 8.4 and 11.5 Jy
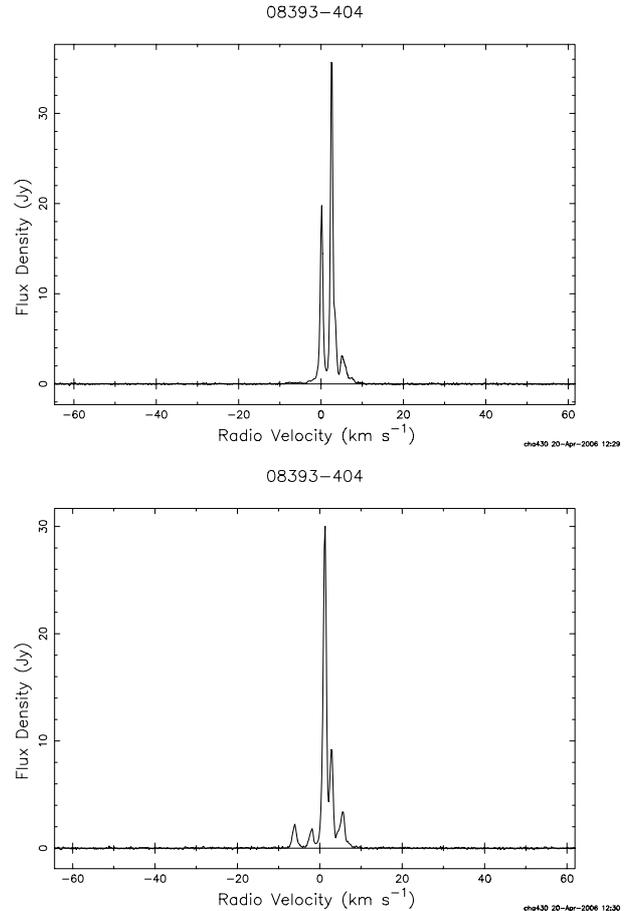
Fig. 1. Spectra of BRC 55 obtained in June 2003 (*top*) and August 2003 (*bottom*).

at $V_{LSR} = -17$ km s^{-1}, close to the cloud systemic velocity ($V_{cl} = -18$ km s^{-1}, see Table 3). Note the remarkable variability of all the spectral features in just 20 days. Weaker emission features appear at either side of the main emission, suggesting that they originate in high velocity outflowing gas, possibly in jet-like structures. The total luminosity of the maser emission is $L(H_2O) = 3.7 \times 10^{-6}$ $L_\odot$.

3.3. BRC 66, SFO 66, IRAS 11315–6259

This weak IRAS source ($L_{FIR} = 190$ $L_\odot$, $d = 1.7$ kpc) is associated with IC 2944 and is part of the H II region RCW 62, in the inner border of the Carina nebula. The BRC is illuminated by
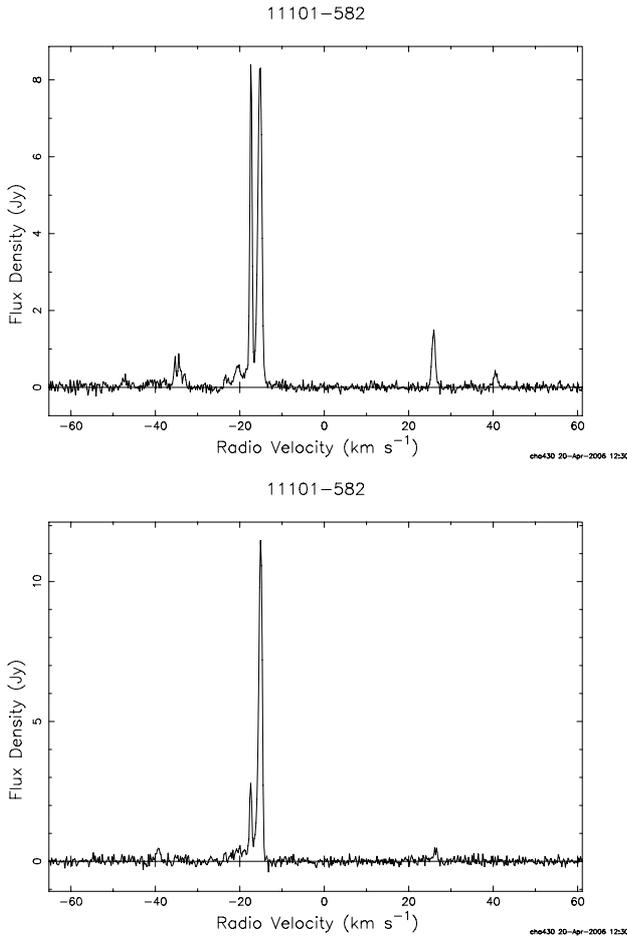
11101−582

11315−625

11101−582

11315−625

Fig. 2. Spectra of BRC 64 obtained on April 10, 2003 (*top*) and April 30, 2003 (*bottom*).
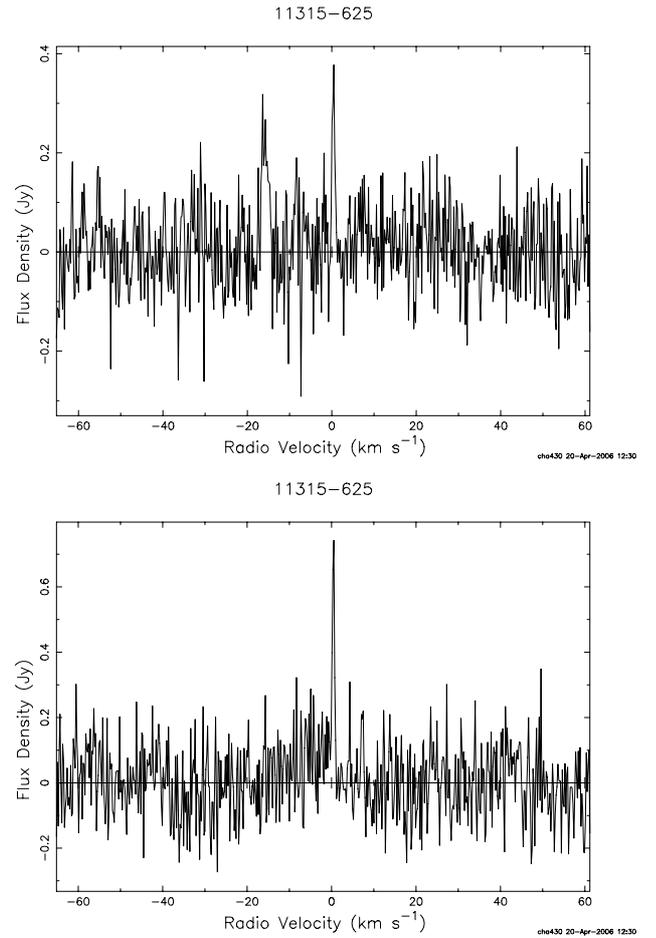
Fig. 3. Spectra of BRC 66 obtained on April 10, 2003 (*top*) and April 30, 2003 (*bottom*).

the O7 III star HD 101131 at projected distance of ∼10 pc. It appears as a prominent rim in the periphery of the large HII region that also hosts the well known Thackeray's dark globules (Reipurth et al. 1997).

The source was observed twice in April 2003 and weak maser emission was detected both times. In the first observation (April 10) the spectrum shown in Fig. 3 displays two features of comparable intensity at $V_{LSR} = 0.5$ km s^{-1} and -16 km s^{-1}, while in the second observation (April 30) the latter component is absent. This feature is quite similar to the cloud velocity $V_{cl} = -17.2$ km s^{-1}. The integrated flux (∼1 Jy km s^{-1}) is the smallest of all the masers detected in this survey. There is no information available in the study of Yamaguchi et al. (1999) on the properties of the molecular cloud associated with this IRAS source, although it is likely the same complex that hosts the nearby BRC 68, also a water maser source but much stronger than BRC 66 (see below). These two YSOs, separated by about 13 arcmin, share a water maser emission at about the same velocity: observations at higher spatial resolution than our single pointing are needed in order to identify the maser position.

3.4. BRC 68, SFO 68, IRAS 11332–6258, G294.5–01.6

This BRC is located in the same region as BRC 66, at the top of a long, filamentary cloud. Inside the HII region RCW 62 and close to the bright rim, there are 3 bright Hα emission line stars, probably precursors to the star formation activity that is now

taking place inside the BRC. OH and H$_2$O maser was reported by Braz et al. (1989). A methanol maser has been detected by Caswell et al. (1993) at a peak velocity of $V_{CH_3OH} = 11.9$ km s^{-1}, close to the cloud systemic velocity of $V_{cl} = 16.8$ km s^{-1} (see also MacLeod & Gaylard 1992). Radio emission at 3 and 6 cm with flux density of 32.4 and 149 mJy, respectively, has been detected by Thompson et al. (2004) in correspondence of the optical rim.

The source was observed only once on April 2003. It has the strongest emission in our sample (peak flux of ∼380 Jy at $V_{H_2O} = -12.6$ km s^{-1}) with multiple components over a velocity interval of ∼13 km s^{-1} (see Fig. 3). Braz et al. (1989) detected a rather intense feature (∼90 Jy) at the same velocity of our strongest component. The total H$_2$O luminosity, $L_{H_2O} = 3.2 \times 10^{-5}$ $L_\odot$, is the largest of the detected maser sources, exceeding the others by factors of 10 to 200.

3.5. BRC 71, SFO 71, IRAS 13050–6154, G304.9+00.5

This moderately bright IRAS source ($L_{FIR} = 1500$ $L_\odot$) is associated with the HII region RCW 75 and is part of the Cen R1 association at a distance of 2.0 kpc (Yamaguchi et al. 1999). The BRC is the top of an elephant trunk cloud that points in the direction of the open cluster Stock 16 (Turner 1985). No radio emission at 3 and 20 cm at an rms level of 7.1 and 4.1 mJy/beam was detected by Thompson et al. (2004).
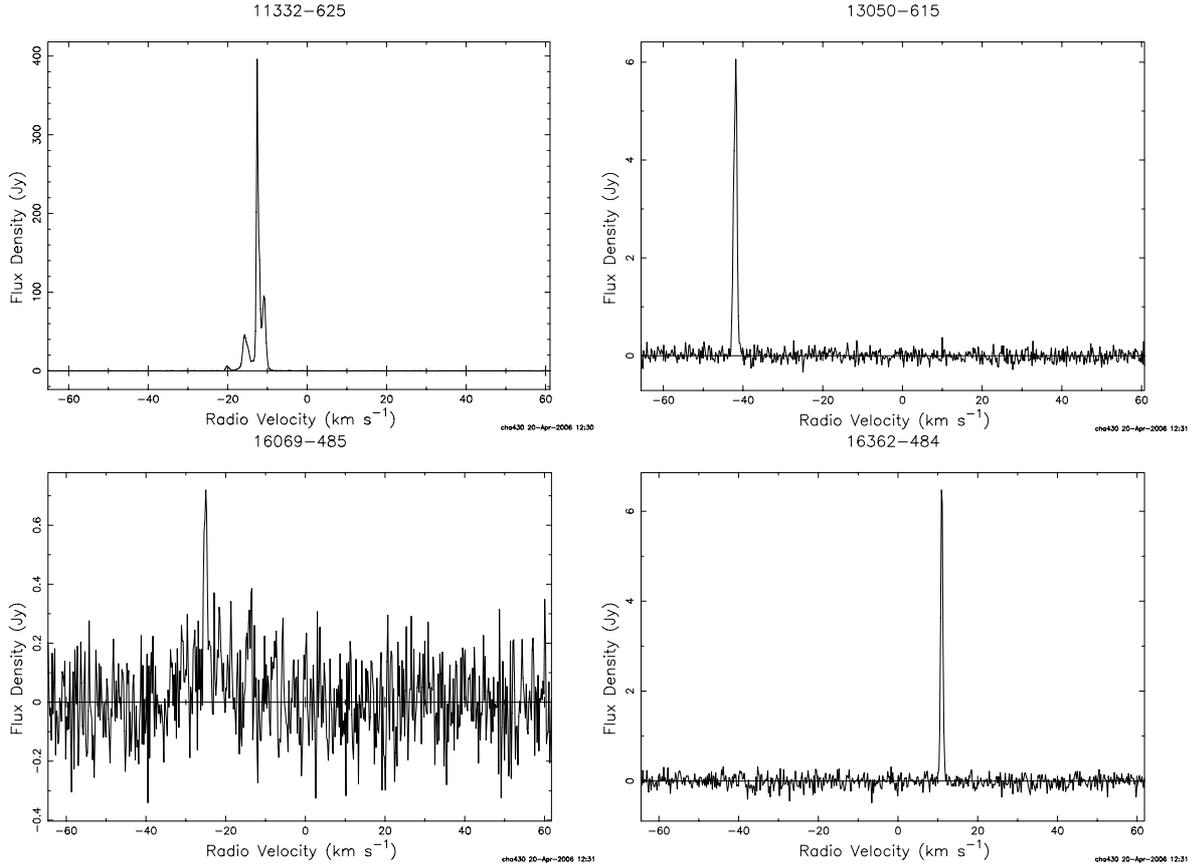
Fig. 4. Spectra of BRC 68 (*top left*), BRC 71 (*top right*), BRC 76 (*bottom left*) and BRC 79 (*bottom right*).

The source was observed only once on April 2003. As shown in Fig. 4, the spectrum has a single narrow and weak component at $V_{H_2O} = -42$ km s^{-1}, offest relative to the systemic cloud velocity of $V_{cl} = -34$ km s^{-1}.

3.6. BRC 76, SFO 76, IRAS 16069–4858, G333.1+01.7

This moderately bright IRAS source ($L_{FIR} = 5600\ L_\odot$, $d = 1.8$ kpc) is associated with the HII region RCW 105, excited by the O7 star HD 144918 (Yamaguchi et al. 1999). The IRAS source is embedded in a small CO cloud with a steep gradient toward the HII region. Intense radio emission at 3 and 6 cm (flux density of 130.4 and 400 mJy, respectively) has been detected by Thompson et al. (2004), in correspondence of the optical rim. Dutra et al. (2005) find evidence for the presence of an embedded IR cluster.

The source has been observed once in May 2005. Together with BRC 66, this is the weakest maser emission, with a six-sigma peak flux density of 0.72 Jy and an integrated flux of ~2 Jy km s^{-1}. The spectrum in Fig. 4 shows a single feature at $V_{H_2O} = -25$ km s^{-1}, coincident with the cloud systemic velocity (see Table 3).

3.7. BRC 79, SFO 79, IRAS 16362–4845, G336.5–01.5

A moderately bright IRAS source ($L_{FIR} = 4400\ L_\odot$, Sugitani & Ogura 1994) associated with the HII region RCW 108, excited by the twin O stars HD 150135 (O5 III) and HD 150136 (O6.5 V), the brightest members of the NGC 6193 cluster in the Ara OB1 association at a distance of 1.35 kpc (Yamaguchi et al. 1999). It is close to another, but weaker IRAS source

(IRAS 16362–4841), embedded in the same cloud which has the highest column density of the Yamaguchi et al. (1999) survey. Interestingly, both IRAS sources have FIR colors consistent with the presence of an ultracompact HII region. However, for unknown reasons, IRAS 16362–4845 was not included in the original list of Sugitani et al. (1991).

Recent observations by Thompson et al. (2004) show that BRC 79 is a strong radio source detected at 3 and 6 cm (flux density of 4.8 and 6.0 Jy, respectively), away from the optical rim and within the cloud core. High resolution observations of the continuum emission and of the H92α recombination line have revealed the presence of a resolved ultracompact HII region, with an integrated radio flux corresponding to that of an O9 ZAMS star (Urquhart et al. 2004). On the basis of 2MASS data, Urquhart et al. (2004) identify nine YSOs within the boundaries of the UC HII region, the central part of the infrared cluster previously noticed by Dutra et al. (2003).

Prior to our observations, water and methanol maser emission has been searched without detection (Braz et al. 1989; MacLeod & Gaylard 1992). We have observed BRC 79 once in May 2005. The spectrum in Fig. 4 displays a single feature at $V_{H_2O} = 11$ km s^{-1}, at a large offset from the cloud systemic velocity of $V_{cl} = -22$ km s^{-1}.

4. Discussion of the maser properties

The sensitive survey ($1\sigma \sim 85$–130 mJy) with the Tidbinbilla 70-m antenna of the 44 southern BRCs listed by Sugitani & Ogura (1994) resulted in the detection of 7 water maser sources, 5 of them for the first time. The location of the 44 southern BRCs in the FIR color–color diagram is shown in Fig. 5.
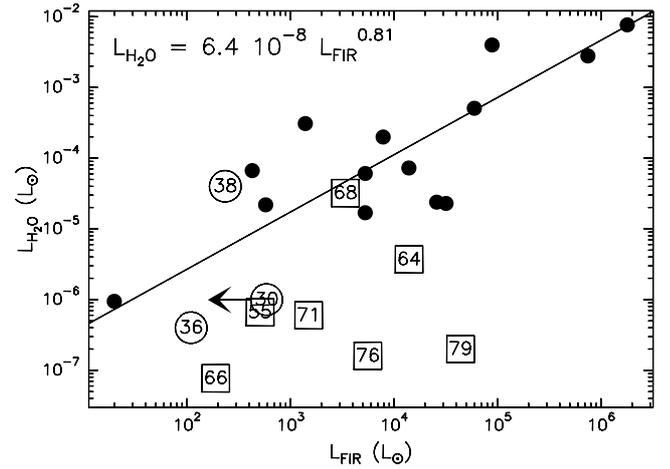
Table 3. Properties of the BRCs with H_2O maser emission.

#	SFR	IRAS	d (kpc)	L_{FIR} ($L_\odot$)	V_{cl} (km s^{-1})	L_{H_2O} ($L_\odot$)
55	Vela MR	08393−4041	0.7	5.1×10^2	+7.6	6.6×10^{-7}
64	BBW 347	11101−5829	2.7	1.4×10^4	−18.4	3.7×10^{-6}
66	RCW 62	11315−6259	1.7	1.9×10^2		7.7×10^{-8}
68	RCW 62	11332−6258	1.7	3.4×10^3	−16.8	3.2×10^{-5}
71	Cen R1	13050−6154	2.0	1.5×10^3	−34.2	6.0×10^{-7}
76	RCW 105	16069−4858	1.8	5.6×10^3	−24.6	1.6×10^{-7}
79	RCW 108	16362−4845	1.4	4.4×10^4	−22.5	2.0×10^{-7}
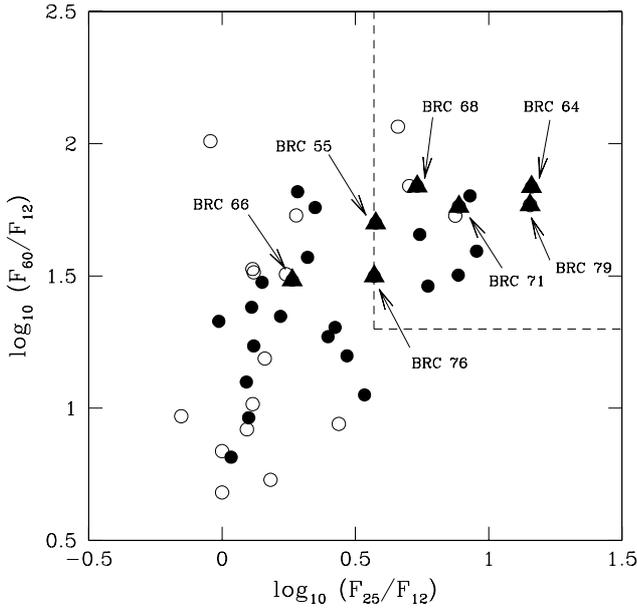
Fig. 5. Location of the southern 44 BRCs in the IRAS color–color diagram. Solid dots represent sources with good IRAS fluxes, while those with upper limits on at least one of the IRAS fluxes are shown as empty circles. The dashed lines delimit the boundaries of UC HII regions proposed by Wood & Churchwell (1989). The H_2O maser sources are shown by the filled triangles.

Fig. 6. Far-infrared vs. H_2O luminosity for the sample of southern (large squares) and northern (large circles) BRCs. The numbers identify the BRC, see Table 1 here and in Valdettaro et al. (2003). The filled circles represent the 14 masers associated with YSOs monitored for 13 years by Brand et al. (2003) and the solid line is a least-squares fit to these data points only.

The dashed lines demarcate the region in the upper right corner occupied by ultracompact HII regions proposed by Wood & Churchwell (1989, hereafter WC). While only 13/44 BRC fall within these boundaries, 6 out of the 7 detected maser sources are located there, yielding a detection rate of ∼50%. The exception is BRC 66 which is also the weakest water maser detected and the least studied of the BRC sample of Yamaguchi et al. (1999). Conversely, the lack of maser emission from BRCs with colors outside of the WC box is significant, with only one detection out of 31 sources. This trend confirms previous results on a high incidence of maser emission from sources with very-red FIR colors and a much lower percentage outside the WC box (Wouterloot & Walmsley 1986; Palla et al. 1991, 1993).

Compared to the results of the less sensitive Medicina survey of the 44 northern BRCs of Sugitani et al. (1991) that resulted in the detection of only 3 masers, we find a detection rate twice as high although the FIR luminosity distribution is basically the same in the two samples. The difference can be accounted for by the higher sensitivity of the Tidbinbilla telescope: three southern BRCs have been detected with a flux density below ∼5 Jy, corresponding to the 3σ detection limit of the Medicina survey. However, the maser emission properties are quite similar in the two samples. For the 10 sources detected in the two surveys, five

are characterized by a small number of emission components extended over a narrow velocity interval (∼1–5 km s^{-1}), while the other five show multiple features covering a velocity interval >10 km s^{-1}. BRC 64 stands out for its extremely large interval of emission velocity (∼100 km s^{-1}). Conversely, BRC 79 which is associated with a UCHII region (Urquhart et al. 2004), has a very weak maser, an atypical result for a massive star.

Figure 6 shows the position of the 7 southern BRCs with water maser emission (numbered squares) in the plot of FIR vs. H_2O luminosity. The figure also includes the 3 water masers detected in the Medicina survey (numbered circles; Valdettaro et al. 2005), along with the 14 sources that have been monitored for up to 13 years at Medicina and that cover a large range of FIR luminosities (Brand et al. 2003). We see that, apart from BRC 68, the northern and southern BRC sources fall below the best fit line found by Brand et al. (2003). Note that the correlation by Brand et al. is based on values of the maser maximum luminosity computed using all the spectra obtained during the long time monitoring campaign which provides a more significant estimate of the true output of the source than the instantaneous values of single or few epoch observations as in the case of both the northern and southern BRC surveys. There are at least two possible explanations, not mutually exclusive, for the observed trend: (1) the correlation does not hold for single epoch observations; (2) the FIR luminosity represents an overestimate of the actual values of the exciting source. The first possibility is partially supported by the fact that water maser emission is highly variable and episodic

(e.g., Claussen et al. 1996; Valdettaro et al. 2003; Furuya et al. 2003), thus obscuring any possible physical correlation existing between the luminosity of the YSO powering the maser and the maser luminosity. For example, Wouterloot et al. (1995) showed that at constant L_{FIR} the water maser luminosity can vary up to four orders of magnitude, based on few observations of a large statistical sample.

Alternatively, one can assume that the contribution of the warm dust heated by the UV radiation field and located inside the bright rim represents a substantial fraction of the observed IRAS fluxes. Then, the intrinsic luminosity of the exciting sources of water maser might be (much) smaller than the values plotted in the figure and the data points would correspondingly shift towards the correlation line. Note that this is not the case of the data points of Brand et al. (2003) that refer to other types of star forming clouds. We favor this interpretation to explain the lack of a correlation. The fact that stellar groups rather than isolated or few stars are found from optical and near-infrared studies of the embedded population of BRCs (e.g., Sugitani et al. 1995; McCaughrean & Andersen 2002; Ogura et al. 2002; Matsuyanagi et al. 2006) confirms the suggestion that the sources exciting water maser emission are of low luminosity (hence, mass).

5. Conclusions

The main result of our surveys of northern and southern BRCs is that only a minor fraction of them shows water maser emission, which is a reliable diagnostic of the presence of very young embedded objects. Does this result imply that star formation is a rare event within these units, contrary to the commonly accepted view of enhanced (or triggered) activity? The limited sensitivity and time coverage of our surveys does not allow to draw a firm conclusion based only on the frequency of occurrence of water masers. However, we can address the question by considering the results of the radio continuum surveys of all the 89 BRCs carried out by Thompson et al. (2004) and Morgan et al. (2004). These studies were aimed at determining the pressure conditions across the ionised boundary layers of the BRCs for comparison with the mean internal pressure in the dense molecular gas. In most cases, it is found that clouds are likely in a state close to pressure equilibrium whereby the photoionisation induced shock can propagate and compress the molecular gas. On the other hand, clear signs of pressure imbalance are found only in a small number of clouds, which could be undergoing gravitational collapse. For example, Urquhart et al. (2006) find BRC 58 and BRC 68 in a state of post-pressure balance and indeed their embedded sources drive both molecular outflows and water masers. Conversely, BRC 76 that appears to be in a pre-pressure balance condition but without sign of ongoing star formation according to Urquhart et al. (2006) was found to have a water maser in our study.

Thus, while the evidence for recent or ongoing star formation is generally present in BRCs, supporting the original idea of active birth sites of Sugitani and collaborators, the empirical evidence for a mode that favors the formation of more massive stars is still lacking (see also Healy et al. 2004). We conclude that the main effect of the propagation of ionization fronts inside BRCs is an enhancement of the fragmentation process of pre-existing density inhomogeneities, thus favoring the formation of low-mass stars, either in small groups or moderate clusters, while the presence of a massive star is a much rarer phenomenon, much as in the case of the stellar IMF.

References

Bertoldi, F. 1989, ApJ, 346, 735
Brand, J., Cesaroni, R., Comoretto, G., et al. 2005, Ap&SS, 245, 133
Braz, M. A., Gregorio Hetem, J. C., Scalise, E., Jr., et al. 1989, A&AS, 77, 465
Caswell, J. L., Gardner, F. F., Norris, R. P., et al. 1993, MNRAS, 260, 425
Cesaroni, R. 2005, Ap&SS, 295, 5
Churchwell, E., Wood, D. O. S., Felli, M., & Massi, M. 1987, ApJ, 321, 516
Dutra, C. M., Bica, E., Soares, J., & Barbuy, B. 2003, A&A, 400, 533
Felli, M., Palagi, F., & Tofani, G. 1992, A&A, 255, 293
Furuya, R. S., Kitamura, Y., Wootten, A., Claussen, M. J., & Kawabe, R. 2001, ApJ, 559, L143
Furuya, R. S., Kitamura, Y., Wootten, A., Claussen, M. J., & Kawabe, R. 2003, ApJS, 144, 71
Georgelin, Y. M., Amram, P., Georgelin, Y. P., le Coarer, E., & Marcelin, M. 1994, A&AS, 108, 513
Goddi, C., & Moscadelli, L. 2006, A&A, 447, 577
Goddi, C., Moscadelli, L., Alef, W., & Brand, J. 2005, A&A, 420, 929
Healy, K. R., Hester, J. J., & Claussen, M. J. 2004, 610, 835
Leung, C. M. 1985, Protostars and Planets II (University of Arizona Press), 104
MacLeod, G. C., & Gaylard, M. J. 1992, MNRAS, 256, 919
Massi, M., Churchwell, E., & Felli, M. 1988, A&A, 194, 116
Massi, F., Giannini, T., Lorenzetti, D., et al. 1999, A&AS, 136, 471
Matsuyanagi, I., Itoh, Y., Sugitani, K., et al. 2006, PASJ, 58, L29
McCaughrean, M. J., & Andersen, M. 2002, A&A, 389, 513
Morgan, L. K., Thompson, M. A., Urquhart, J. S., White, G. J., & Miao, J. 2004, A&A, 426, 535
Moscadelli, L., Cesaroni, R., & Rioja, M. J. 2005, A&A, 438, 889
Ogura, K., & Walsh 1992, ApJ, 400, 248
Ogura, K., Sugitani, K., & Pickles, A. 2002, AJ, 123, 2597
Palla, F., Brand, J., Comoretto, G., Felli, M., & Cesaroni, R. 1991, A&A, 246, 249
Palla, F., Cesaroni, R., Brand, J., et al. 1993, A&A, 280, 599
Reipurth, B. 1983, A&A, 117, 183
Reipurth, B., Corporon, P., Olberg, M., & Tenorio-Tagle, G. 1997, A&A, 327, 1185
Staveley-Smith, L. G. 1985, Ph.D. Thesis, University of Manchester
Sugitani, K., Fukui, Y., & Ogura, K. 1991, ApJS, 77, 59
Sugitani, K., & Ogura, K. 1994, ApJS, 92, 163
Sugitani, K., Tamura, M., & Ogura, K. 1995, ApJ, 455, L39
Tamura, M., Hough, J. H., Chrysostomou, A., et al. 1997, MNRAS, 287, 894
Tauber, Jan A., Lis, Dariusz C., & Goldsmith, Paul F. 1993, ApJ, 403, 202
Thompson, M. A., Urquhart, J. S., & White, G. J. 2004, A&A, 415, 627
Trinidad, M. A., Rojas, V., Plasencia, J. C., et al. 2003, RMxAA, 39, 311
Turner, D. G. 1985, ApJ, 292, 148
Urquhart, J. S., Thompson, M. A., Morgan, L. K., & White, G. J. 2004, A&A, 428, 723
Urquhart, J. S., Thompson, M. A., Morgan, L. K., & White, G. J. 2006, A&A, 450, 625
Valdettaro, R., Palla, F., Brand, J., et al. 2002, A&A, 383, 244
Valdettaro, R., Palla, F., Brand, J., & Cesaroni, R. 2005, A&A, 443, 535
Yamaguchi, R., Saito, H., Mizuno, N., et al. 1999, PASJ, 51, 791
Walsh, A. J., Hyland, A. R., Robinson, G., & Burton, M. G. 1997, MNRAS, 291, 261
Wood, D. O. S., & Churchwell, E. 1989, ApJ, 340, 265
Wouterloot, J. G. A., & Walmsley, C. M. 1986, A&A, 168, 237
Wouterloot, J. G. A., Fiegle, K., Brand, J., & Winnewisser, G. 1995, A&A, 301, 236 (Erratum: 1997, A&A, 319, 360)